

# MetricHMR: Metric Human Mesh Recovery from Monocular Images

He Zhang<sup>\*1</sup>, Chentao Song<sup>\*1</sup>, Hongwen Zhang<sup>†2</sup>, Tao Yu<sup>†1</sup>  
<sup>1</sup>Tsinghua University, <sup>2</sup>Beijing Normal University

## Abstract

We introduce *MetricHMR (Metric Human Mesh Recovery)*, an approach for metric human mesh recovery with accurate global translation from monocular images. In contrast to existing HMR methods that suffer from severe scale and depth ambiguity, *MetricHMR* is able to produce geometrically reasonable body shape and global translation in the reconstruction results. To this end, we first systematically analyze previous HMR methods on camera models to emphasize the critical role of the standard perspective projection model in enabling metric-scale HMR. We then validate the acceptable ambiguity range of metric HMR under the standard perspective projection model. Finally, we contribute a novel approach that introduces a ray map based on the standard perspective projection to jointly encode bounding-box information, camera parameters, and geometric cues for End2End metric HMR without any additional metric-regularization modules. Extensive experiments demonstrate that our method achieves state-of-the-art performance, even compared with sequential HMR methods, in metric pose, shape, and global translation estimation across both indoor and in-the-wild scenarios.

## 1. Introduction

Human mesh recovery (HMR) from a single image [2, 3, 5, 8, 13] is an attractive task because of its wide range of applications, such as movie making, game making, AR / VR, and motion analysis.

Most existing HMR methods [2–5, 8, 10, 13, 22, 37, 38] do not consider metric properties because the intrinsic parameters of the images in the wild are often unknown. Therefore, to enable the network to uniformly process different images, previous methods could only use a fixed weak perspective projection model (approximately orthographic projection). Although this approach circumvents the limitation of unknown intrinsic parameters, the size of the object’s projection in a weak perspective projection model is not affected by changes in depth. In other words,

regardless of the person’s location or shape, their 2D projection in the image remains approximately invariant. Therefore, existing methods struggle to estimate the metric shape, global 3D position, and trajectory, making it difficult to perform the metric HMR estimation.

Estimating the human global mesh (not only including pose and shape, but also global rotation and translation) has always been a key focus of HMR research. CLIFF [14] carries location information in full frames, addressing the issue of how the person’s global orientation should change with the position of the bounding box (Bbox). Methods such as TRACE [26], WHAM [24], and GVHMR [23] attempt to incorporate additional trajectory regression modules to recover global 3D position. These methods have demonstrated promising results. However, these still cannot be considered metric HMR methods, as they are based on a weak perspective model, which cannot perceive the metric body shape and the distance relationship between the human body and the camera. Therefore, their 3D position is heavily dependent on the trajectory regression module.

In real-world applications, it is required to recover the real 3D position of the human body and a human body with real scale, rather than just aligning with 2D observations. Metric does not mean absolute accuracy; rather, it represents that the recovery results are reasonable in scale. To achieve this, the HMR network needs to discard the uniform fixed weak perspective assumption and possess the ability to perceive different camera projection parameters.

In this work, our key observation is that, with the perspective projection camera parameters known, the network can better perceive the depth of the human body, thereby determining the real scale of a human. In perspective projection, the camera focal length and translation in the depth direction of the human body determine the projection scale on the 2D plane, while the camera principal point and translation in other directions determine the projection location. If the camera parameters are known, it is possible to circumvent the issues introduced by weak perspective projection and accurately perceive the real 3D location.

In this paper, we propose *metricHMR* for metric human mesh recovery from monocular images. We first analyze in detail the relationship between the 3D position of the human

<sup>\*</sup>Equal contribution.

<sup>†</sup>Corresponding author.



Figure 1. **MetricHMR: Metric Human Mesh Recovery.** MetricHMR can achieve metric shape, pose and global translation estimation, enabling 3D scene mesh overlay (left) and global trajectory estimation (right) from monocular images.

mesh and the 2D image, investigate the corresponding pose ambiguities under perspective projection. Then, taking the cropped image as input, we introduce the camera ray representation method to comprehensively describe camera parameters and the bounding box. Finally, we use camera ray conditioned 3D human mesh regression to regress the 3D human mesh. Unlike existing methods [2, 8, 10, 13] that ensure overlay by estimating the camera’s translation, we directly estimate the real position of the human body in the camera coordinate system. Standard perspective projection and camera parameters ensure the recovery of the metric human mesh, even without any supervision of 3D information during the training process.

Moreover, existing state-of-the-art single-image depth estimation approaches have demonstrated that it is possible to recover 2.5D information with physical scales by integrating semantic and scale priors. Such approaches could be incorporated with the proposed MetricHMR. Since the human visual system itself is a standard perspective projection model, the emergence of such methods [20, 21, 34, 36] allows us to explore whether we can achieve a more human-perceptive HMR under the guidance of relatively accurate camera intrinsics.

In summary, our contributions are as follows:

- We introduce MetricHMR for human mesh recovery from monocular images with metric awareness. Using camera rays to represent camera parameters and bounding boxes, and incorporating them as conditions for the regressor, MetricHMR can recover the metric shape and 3D position without requiring any 3D information as training supervision.
- We systematically analyze existing global trajectory-

aware HMR methods and conduct an in-depth analysis of the impact of camera models on metric estimation. Our analysis identifies the most critical component in the formulation of perspective projection. Such insights make the proposed method simple yet effective.

- We integrate state-of-the-art monocular depth estimation techniques with MetricHMR to handle the challenge of in-the-wild scenarios. Experimental results demonstrate superior performances on indoor and in-the-wild datasets.

## 2. Related Work

### 2.1. Human Mesh Recovery

Estimating human pose and body shape (HPS) from a single image is a classic task that has been studied extensively with both optimization-based and regression-based methods. Optimization-based methods are among the earliest and best-studied approaches. These methods [2, 6, 19, 33] usually fit a parametric model to the 2D keypoints of the image. Regression-based methods [3–5, 8, 10, 14, 37, 38] usually directly regress parametric models from images. Due to the unknown camera parameters, existing methods can only assume a weak perspective projection model with a fixed focal length. However, under the weak perspective projection assumption, the object’s projection does not change with depth and shape, making it difficult to estimate the metric properties of the human body, such as metric shape and global 3D positions.

To better estimate human shape, pose, and 3D position, existing methods primarily focus on two improvements: constructing more accurate camera models or adding additional 3D position/trajectory modules. Tab. 1 shows some

Table 1. Comparison of our method with other related works.

| Method       | Input     | Camera Model                  | Trajectory Module         | 3D loss | 3D pose |
|--------------|-----------|-------------------------------|---------------------------|---------|---------|
| HMR [8]      | per-frame | $f_{crop} = 5000.$            | ✗                         | ✓       | ✗       |
| SPIN [13]    | per-frame | $f_{crop} = 5000.$            | ✗                         | ✓       | ✗       |
| PyMAF [37]   | per-frame | $f_{crop} = 5000.$            | ✗                         | ✓       | ✗       |
| HMR2.0 [5]   | per-frame | $f_{crop} = 5000.$            | ✗                         | ✓       | ✗       |
| CLIFF [14]   | per-frame | $f_{full} = \sqrt{W^2 + H^2}$ | ✗                         | ✓       | ✗       |
| Zolly [31]   | per-frame | $f_{crop} = shz/2$            | ✗                         | ✓       | ✓       |
| SPEC [11]    | per-frame | Predicted focal, pitch, roll  | ✗                         | ✓       | ✓       |
| SLAMHMR [35] | temporal  | $f = (W + H)/2$               | Optimization              | ✓       | ✓       |
| TRACE [26]   | temporal  | $f = 443.4$                   | BVE                       | ✓       | ✓       |
| GVHMR [23]   | temporal  | $f_{full} = \sqrt{W^2 + H^2}$ | Gravity-View system       | ✓       | ✓       |
| WHAM [24]    | temporal  | $f_{full} = \sqrt{W^2 + H^2}$ | Decoder                   | ✓       | ✓       |
| TRAM [32]    | temporal  | Ground truth $K$              | Coordinate transformation | ✓       | ✓       |
| MetricHMR    | per-frame | Ground truth/Unidepth $K$     | No need                   | No need | ✓       |

representative methods.

In terms of camera model improvements, Sun et al. [25, 26] discards the conventional fixed value of 5000 and opts for a smaller focal length, enhancing the 3D position perception. SLAMHMR [35] takes the average of the image height  $H$  and width  $W$  as the focal length. CLIFF [14] developed a new global focal length  $f_{full}$  calculation method, defined as  $f_{full} = \sqrt{W^2 + H^2}$ . This approach has also been adopted in GVHMR [23] and WHAM [24]. SPEC [11] designs a network to predict the camera’s focal length, pitch, and roll. Zolly [31] estimates human depth using camera distortion and then calculates the focal length as  $f_{crop} = shz/2$ , where  $s$  is the scale,  $h$  is the height of the cropped image,  $z$  is the human depth. While the above methods have achieved satisfactory performance, the modeling of the camera still differs from the actual camera projection. TRAM [32] directly employs standard perspective projection and uses the ground truth intrinsic parameters of the image for projection. It has achieved excellent results across multiple datasets, demonstrating the strong potential of perspective projection.

To estimate the 3D position and trajectory of the human body, many methods tend to incorporate a related module. Sun et al. [25, 26] introduce the Bird’s Eye View module to infer 3D body position. SLAMHMR [35] uses DORID-SLAM [27] to estimate camera pose and introduces an optimization module to get 3D motion trajectory. WHAM [24] incorporates a decoder to regress global trajectory. TRAM [32] uses a coordinate transformation to convert the 3D positions estimated from cropped images into a global trajectory. These methods have indeed achieved good results; however, we are curious if there is a way to directly regress the global position and motion trajectory without the need for additional module support.

Through analysis, we believe that the limitations in metric shape, pose and 3D position estimation are due to discrepancies between the assumed camera model and the real camera model. Therefore, we propose a simple yet effective method: MetricHMR. This method uses standard perspective projection to estimate metric shape, pose, and 3D position without the need for temporal input, additional module design, or supervision of 3D.

## 2.2. Metric Depth

The development of metric depth estimation has brought new opportunities and inspirations to human pose estimation. ZeoDepth [1] introduces the metric bins module to ensure metric depth. Metric3D [36] uses large-scale data and canonical camera transformation to train a zero-shot metric depth model. Zhao et al. [39] proposed MfH, in which they use HMR2.0 [5] to estimate the shape of painted humans as a reference for metric depth estimation. However, HMR2.0 itself is not a human mesh recovery method in metric terms, resulting in limited accuracy. UniDepth [21] uses the angular map to describe camera parameters and introduces a pseudo-spherical representation of the output space to disentangle camera parameters and metric depth. SharpDepth [20] combines UniDepth and a diffusion-based depth estimator to obtain detailed metric depth. DepthAnythingV2 [34] fine-tunes with metric depth labels to obtain its metric depth models.

These methods has provided new support for human mesh recovery. BLADE [30] uses DepthAnythingV2 to estimate the pelvis depth of the person near the camera to solve the accurate focal length and full 3D translation. TRAM [32] uses ZeoDepth to estimate the metric scale of humans. However, directly using the estimated depth as inputs may limit such human mesh recovery methods to the

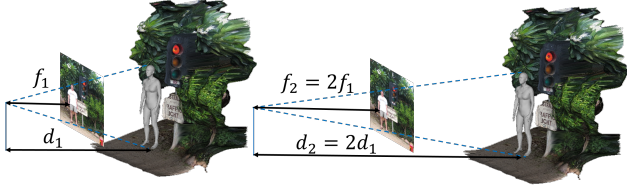


Figure 2. Illustration of the human body’s metric distance under the same 2D projection with different focal lengths. Focal:  $f$ , distance:  $d$ .

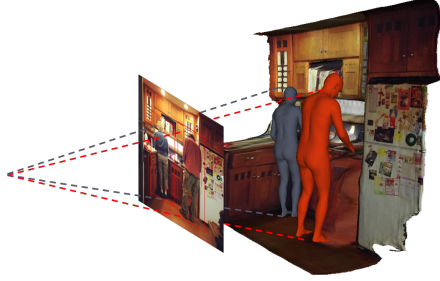


Figure 3. Illustration of the human body’s metric position with different bounding box. The position of the bounding box directly influences the 3D location of the human body.

accuracy of the depth estimation.

### 3. Metric Pose Bias

#### 3.1. Camera and Image

The intrinsic parameters of an image and depth can be obtained by understanding the scene and image. In recent years, some methods [21, 34, 36] have achieved the estimation of intrinsic parameters and metric depth through training on large amounts of metric data. Under this premise, metric human mesh recovery becomes possible.

When discussing the metric human mesh recovery in the camera coordinate system of perspective projection, the human body’s real scale and 3D position are closely related to the camera intrinsics and the projection on the 2D plane. Fig.2 shows the impact of the camera’s intrinsic parameters on the metric depth of the human body. If two cameras ( $f_2 = 2f_1$ ) produce the same image size for the same person, their metric depths are different ( $d_2 = 2d_1$ ). If the focal length can be provided as a known parameter to the network, it becomes possible for the network to infer the metric depth of the human body.

The distance of the principal point ( $c_x, c_y$ ) and the position of the human body in the 2D projection reflect the metric movement of the human body in the 3D space. The principal point is usually located within a certain range near the center of the image. Similarly to CLIFF [14], we introduce the bounding box information to represent the position of the cropped human image within the entire image. How-

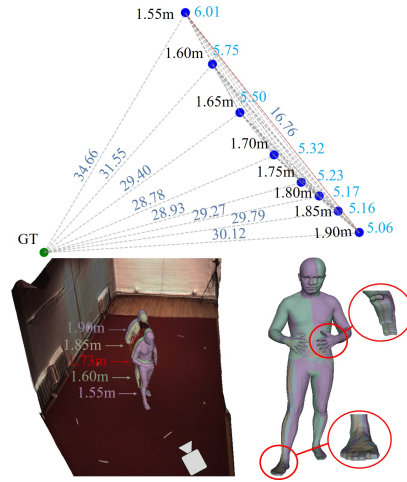


Figure 4. Ambiguity. Upper: quantitative comparison. The green point represents the ground truth, while the blue points represent the solutions. PA-MPJPE is marked as glaucous. Mean 2D key-points errors are marked as light blue. The red lines indicate the two solutions with the largest differences. Bottom left: the ambiguity of global translation. Different shapes correspond to varying depths (subject’s metric point cloud: red). Bottom right: a qualitative comparison of pose ambiguity.

ever, unlike CLIFF, which uses the bounding box to determine the global rotation of the human body, we use it to assess the 3D metric position of the human body, as shown in Fig.3.

#### 3.2. Pose Ambiguity

Pose ambiguity is another well-known issue. The lack of constraints in a single image and the weak perspective projection assumption make it difficult for existing methods to estimate the metric scale and depth of the human body. For perspective projection, when the camera parameters are known, either the metric body shape or the global position of the human body can determine the other. However, this does not imply that the solution is absolutely accurate and unique. We designed an experiment to illustrate this issue.

Following SMPLify-XMC [18], we use mimic loss, 2D loss, and measurement loss to solve human pose and shape. Measurement loss is used to condition the solution under different heights. Fig.4 (upper) shows different solutions at different body heights. The ground truth is marked as the green point. The PA-MPJPE (Procrustes-aligned Mean Per Joint Position Error) is marked as glaucous. Mean 2D key-point errors are marked as light blue. It can be observed that, although the mean 2D keypoint errors among the solutions under different body heights differ by less than half a pixel, the maximum difference in PA-MPJPE (Procrustes-aligned Mean Per Joint Position Error) between each solution can still reach 16.76mm. Fig.4 further illustrates the

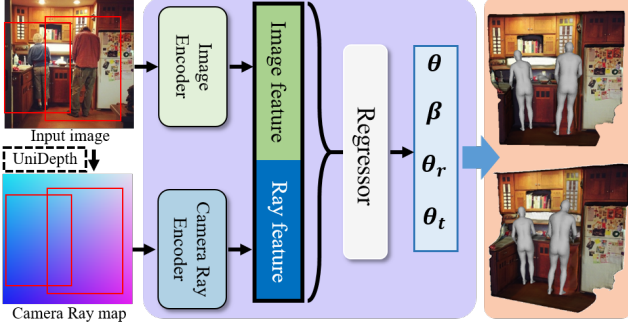


Figure 5. Pipeline. Given a single frame image, MetricHMR first represents the camera parameters as a camera ray map (if the intrinsic parameters are unknown, they are obtained using UniDepth). It incorporates an image encoder and a ray encoder to extract features from the image and ray map, respectively. Finally, a multi-layer perceptron (MLP) regressor is used to obtain the human body’s pose, shape, and 3D position.

ambiguity in 3D global translation (bottom left) and body poses (bottom right) across different heights. In the single-image human mesh recovery task, the solutions can align well with the observations, but there are still notable differences in PA-MPJPE among the solutions. Therefore, the goal of this paper is to recover a reasonable metric human mesh, rather than to achieve a unique absolute result.

## 4. MetricHMR

Based on the previous analysis, we aim to propose a simple yet effective method to simultaneously obtain the pose, shape, and global position of the human body. We use SMPL [16], a linear parametric model, to represent the human body. MetricHMR takes a single RGB image  $I$  as input and outputs the pose parameters  $\theta \in \mathbb{R}^{69}$ , shape parameters  $\beta \in \mathbb{R}^{10}$ , and global rotation  $\theta_r \in \mathbb{R}^3$  and metric translation  $\theta_t \in \mathbb{R}^3$  of the SMPL model. The pipeline is shown in Fig.5.

### 4.1. Camera Ray Representation

In this paper, we use perspective projection to represent the camera model and implement human mesh recovery in the camera coordinate system. As demonstrated in Sec.3, the key factors affecting 3D human mesh recovery are the size of the image, the bounding box, and intrinsic parameters. The above three factors collectively determine the 3D position of the human body in the camera coordinate system. The most intuitive idea is to reference CLIFF [14] and use the bounding box and intrinsic parameters directly as input to the regression network. However, for our task, this CLIFF-like method presents several problems.

First, CLIFF represents the bounding box information

$I'_{bbox}$  as:

$$I'_{bbox} = \left[ \frac{c'_x}{f_{CLIFF}}, \frac{c'_y}{f_{CLIFF}}, \frac{b'}{f_{CLIFF}} \right] \quad (1)$$

where  $f_{CLIFF} = 5000$ .  $c'_x$  and  $c'_y$  are the bounding box locations relative to the full image center, as shown in Fig.6 (left). However, for perspective projection, the principal point is not at the center of the image, and the focal length of the cropped image cannot be assumed to be a fixed value. Secondly, the root translation  $t_{crop}$  (on the cropped image) and the transformed root translation  $t_{full}$  (on the original image) do not represent the metric 3D position. Lastly, it remains unclear how to express the intrinsic parameters of the perspective projection camera in a form suitable for network computation and understanding. If the intrinsic parameters, image size, and other information are directly fed into the network, it will inevitably put pressure on the network’s training and generalization.

To address the aforementioned problems, we propose a camera ray representation method to comprehensively represent the bounding box, intrinsic parameters, and other related information. Given the intrinsic matrix  $K$  of the original image

$$K = \begin{bmatrix} f_x & 0 & c_x \\ 0 & f_y & c_y \\ 0 & 0 & 1 \end{bmatrix}. \quad (2)$$

Each pixel corresponds to a camera ray vector  $d$

$$d = K^{-1}[u, v, 1] \quad (3)$$

where  $(u, v)$  represents the coordinate of the pixel on the image. The camera rays in the bounding box will form a Bbox visual cone (Fig.6 middle). As shown in Fig.6 (right), the direction of the rays in the bounding box includes both the camera parameter information and the bounding box information. Moreover, this representation is invariant to cropping, meaning that cropping the original image will not affect the direction of the rays within the bounding box.

Specifically, for a cropped image,  $K_{crop}$  can be calculated as:

$$K_{crop} = \begin{bmatrix} (f_x - u_{bbox})/s & 0 & c_x/s \\ 0 & (f_y - v_{bbox})/s & c_y/s \\ 0 & 0 & 1 \end{bmatrix}. \quad (4)$$

Then, use Equation (3) to calculate the camera ray bundle corresponding to the cropped image. For images with unknown camera parameters, we utilize UniDepth [21], a metric depth estimation method, to estimate the intrinsics of the camera.

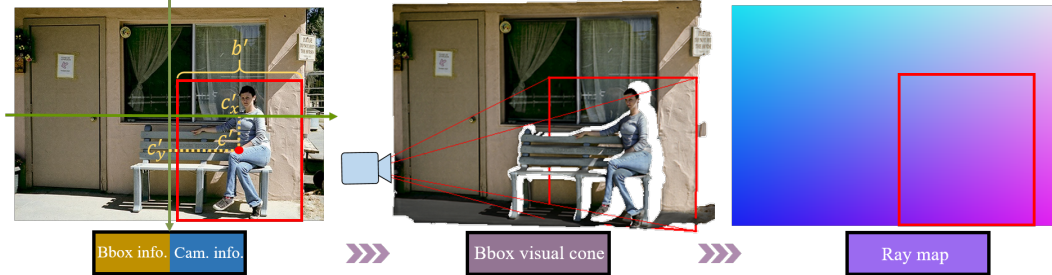


Figure 6. Camera ray representation. Left: bounding box and camera representation in CLIFF. Middle: bounding box visual cone. Right: camera ray representation.

## 4.2. Camera Ray Conditioned 3D Human Mesh Regression

HMR [8] is a simple and classical method for estimating human pose and shape. However, achieving metric shape [30] and 3D trajectory estimation [23, 26, 32] often necessitates the incorporation of additional modules, which inevitably increases the complexity of the overall pipeline. We aim to achieve the above tasks with a simple and effective method, without introducing too many additional modules. Then we proposed camera ray conditioned 3D human mesh regression, as is shown in Fig.5.

Given a single frame image, we obtain the corresponding ray map as described in Sec.4.1. we utilize two distinct vision transformers (ViT) to encode the image and the ray map separately. The image is processed through the image encoder and the camera ray map through the camera ray encoder, yielding the image feature  $I_{feat}$  and the ray feature  $R_{feat}$ . We take an MLP-based iterative error feedback loop [8] as the regressor. The image feature  $I_{feat}$  and the ray feature  $R_{feat}$  are concatenated and fed into a regressor to obtain the parameters of the human mesh. Using the implicit function  $F(\cdot)$  to represent the human mesh recovery process, the entire regression part can be expressed as:

$$\theta, \beta, \theta_r, \theta_t = F(I_{feat}, R_{feat}). \quad (5)$$

As shown in Fig.5, compared to HMR [8], the proposed method only adds the condition of camera rays. This not only allows for the recovery of the human pose and shape but also enables the estimation of the correct 3D position. Moreover,  $\theta_t$  represents the 3D spatial position in the camera coordinate system, eliminating the need for transformations like cropping the image to the whole image as seen in CLIFF [14]. We will further validate the effectiveness of the method in the experimental section.

Losses: We use the mean squared error (MSE) loss in pose mimic loss, shape loss, and 2D keypoints loss. Our whole training process does not require 3D joint loss, which makes the selection of datasets more flexible.

## 5. Experiments

### 5.1. Implementation Details

**Training details.** We trained MetircHMR on 3DPW [29], Human3.6M [7], and MPI-INF-3DPH [17] for 40 epochs with a weight decay of 0.01. During training, we used the AdamW optimizer with a batch size of 64. The learning rate was set to  $1 \times 10^{-6}$  for the pre-trained HMR2.0 backbone, and  $1 \times 10^{-5}$  for the camera ray encoder and the transformer decoder.

**Evaluation and metrics.** We selected different evaluation metrics, for different tasks.

To evaluate human mesh recovery, we introduce PVE (Per Vertex Error), MPJPE (Mean Per Joint Position Error), and PA-MPJPE (Procrustes-aligned Mean Per Joint Position Error).

To evaluate trajectory estimation, Following prior work [12, 24, 32, 35], we adopt WA-MPJPE<sub>100</sub> (World PA Trajectory-MPJPE), W-MPJPE<sub>100</sub> (World PA First - MPJPE), RTE (Root Translation Error), and ERVE (Egocentric-frame Root Velocity Error) as evaluation metrics for assessing global human motion and trajectory accuracy.

Table 2. Quantitative comparisons with state-of-the-art methods on local human body poses. (PA-M.: PA-MPJPE.)

|        | 3DPW(14) |       |      | EMDB-1(24) |       |       |
|--------|----------|-------|------|------------|-------|-------|
|        | PA-M.    | MPJPE | PVE  | PA-M.      | MPJPE | PVE   |
| SPIN   | 44.4     | 69.8  | 82.2 | 60.7       | 98.3  | 120.8 |
| CLIFF  | 43.0     | 69.0  | 81.2 | 68.3       | 103.3 | 123.7 |
| HMR2.0 | 44.5     | 70.0  | -    | -          | -     | -     |
| ReFit  | 41.0     | 65.8  | -    | -          | -     | -     |
| TRACE  | 50.9     | 79.1  | 95.4 | 71.5       | 110.0 | 129.6 |
| WHAM   | 35.9     | 57.8  | 68.7 | 50.4       | 79.7  | 94.4  |
| TRAM   | 35.6     | 59.3  | 69.6 | 45.7       | 74.4  | 86.6  |
| ours   | 37.5     | 60.5  | 72.1 | 52.4       | 87.1  | 104.0 |

## 5.2. Comparisons

**Human mesh recovery estimation.** We first conducted a quantitative comparison of local body poses with state-of-the-art methods on the 3DPW [29] and EMDB-1 [9] datasets. We not only compare our method with per-frame approaches but also with temporal methods. The specific results are shown in Tab.2. Our method, as a per-frame approach, scores slightly lower than the two temporal methods but outperforms similar per-frame methods. This difference is also acceptable because no additional temporal information is used.

**Trajectory estimation.** We further conducted a quantitative comparison of global pose and trajectory estimation. We first compare on EMDB-2 dataset, a dynamic camera setup dataset. Methods adapted for global pose and trajectory estimation with dynamic cameras often incorporate some SLAM methods (DROID [27], DPVO [28]) to estimate the camera motion. Since dynamic camera pose estimation is not the focus of this paper, we compare the results based on SLAM and ground truth camera poses. In this process, we follow TRACE [26] and use Masked-DROID to estimate the camera extrinsic. From Tab.3, it is evident that our method and TRAM are the two best-performing approaches. Our method slightly outperforms TRAM. From the qualitative trajectory comparison in Fig.7, our method aligns better with the ground truth than TRAM.

Table 3. Quantitative comparisons of global trajectory and motion estimation on EMDB, a dynamic camera dataset. (M.D.: Masked DROID. WA-M.: WA-MPJPE<sub>100</sub>. W-M.: W-MPJPE<sub>100</sub>.) RTE is in %, ERVE is in mm/frame, all other errors are in mm.

|                    | EMDB-2 |       |     |      |
|--------------------|--------|-------|-----|------|
|                    | WA-M.  | W-M.  | RTE | ERVE |
| WHAM (w/ DROID)    | 133.3  | 343.9 | 4.6 | 14.7 |
| GVHMR (w/ DPVO)    | 111.0  | 276.5 | 2.0 | -    |
| TRAM (w/ M.D.)     | 76.4   | 222.4 | 1.4 | 10.3 |
| Ours (w/ M.D.)     | 77.0   | 226.0 | 1.4 | 10.1 |
| WHAM (w/ GT gyro)  | 131.1  | 335.3 | 4.1 | 13.7 |
| GVHMR (w/ GT gyro) | 109.1  | 274.9 | 1.9 | -    |
| TRAM (w/ GT extr)  | 62.7   | 182.8 | 0.2 | 9.6  |
| Ours (w/ GT extr)  | 61.3   | 181.4 | 0.2 | 8.9  |

Additionally, we compared our method with TRAM, which performed well on the EMDB dataset, using the Human3.6M, a static camera setup dataset. As shown in Tab.4, the experimental results further demonstrate the effectiveness of our proposed method.

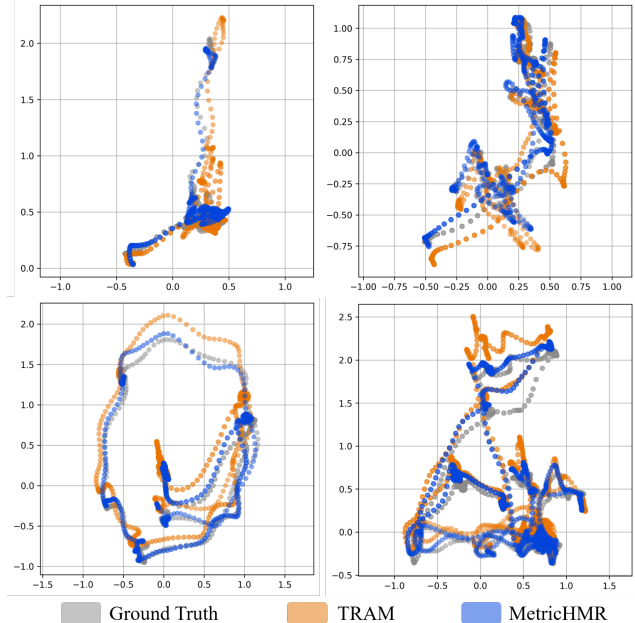


Figure 7. Qualitative comparison of global trajectory estimation on EMDB. Overall, MetricHMR shows better alignment to ground truth data.

Table 4. Quantitative comparisons of global trajectory and motion estimation with TRAM on Human3.6M, a static camera dataset. (WA-M.: WA-MPJPE<sub>100</sub>. W-M.: W-MPJPE<sub>100</sub>.)

|      | Human3.6M |       |     |      |
|------|-----------|-------|-----|------|
|      | WA-M.     | W-M.  | RTE | ERVE |
| TRAM | 76.2      | 129.8 | 0.9 | 13.2 |
| Ours | 72.9      | 114.6 | 0.9 | 12.1 |

**3D overlay with the point cloud.** Fig. 8 illustrates the 3D overlay with the point cloud on in-the-wild data from the COCO dataset [15]. We use Unidepth [21] to estimate the depth map and the intrinsics of the image, thus obtaining the 3D point cloud. MetricHMR accurately estimates the metric body shape and 3D position of humans, allowing the results to be overlaid with the 3D point cloud rather than just being displayed on the 2D image. The results demonstrate the effective recovery of metric 3D human poses and highlight the method’s robustness and accuracy in real-world scenarios.

## 5.3. Ablation Study

In this section, we validate the performance improvement provided by the camera ray representation. The results are shown in Tab.5. (1) Bbox+K: similar to CLIFF, directly incorporates camera intrinsic parameters and bounding box information as additional input to the network. (2) Ray: Our

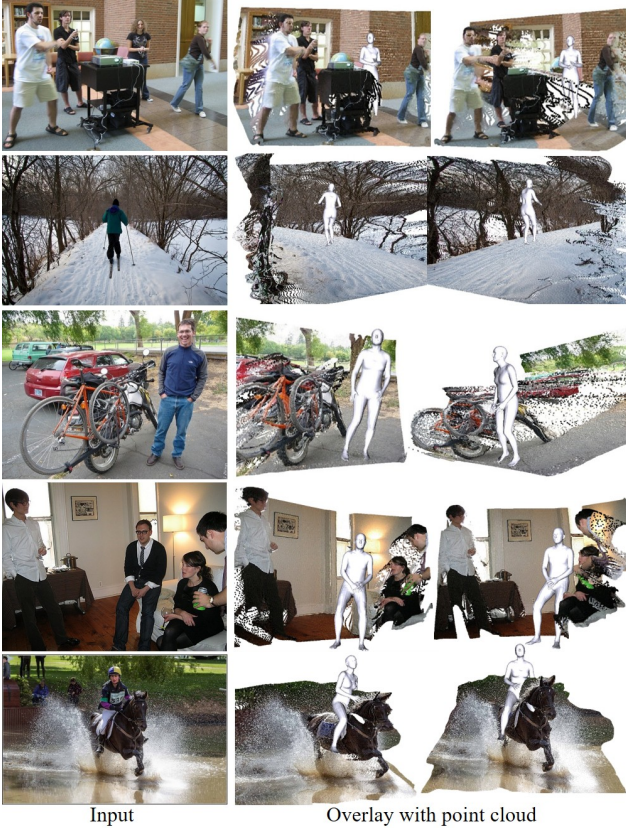


Figure 8. 3D overlay with the point cloud on in-the-wild data from the COCO dataset.

camera ray representation method uses a camera ray bundle to comprehensively represent camera intrinsic parameters and bounding box information. From Tab.5, we can see that the metrics drop significantly, especially in the 3DPW dataset. This is primarily because the network struggles to understand the aforementioned parameters. The diversity of intrinsic parameters poses challenges for the network’s generalization. The experimental results on the 3DPW and H36M datasets demonstrate the effectiveness of the proposed method.

Table 5. Ablation studies (PA-M.: PA-MPJPE).

|        | 3DPW (14)   |             |             | Human3.6M (24) |             |             |
|--------|-------------|-------------|-------------|----------------|-------------|-------------|
|        | PA-M.       | MPJPE       | PVE         | PA-M.          | MPJPE       | PVE         |
| Bbox+K | 80.9        | 111.5       | 129.2       | 42.3           | 74.4        | 91.2        |
| Ray    | <b>37.5</b> | <b>60.5</b> | <b>72.1</b> | <b>37.6</b>    | <b>63.4</b> | <b>68.3</b> |

## 6. Conclusion

In this paper, we introduce MetricHMR, a novel approach for regressing the metric human shape, pose, and 3D position in the camera coordinate system from a single image. MetricHMR uses standard perspective projection to formulate the human mesh recovery problem. It employs a camera ray representation method to comprehensively describe the bounding box information and camera parameters. We utilize a simple pipeline architecture to recover human metric information and 3D position without the need for additional modules, temporal information input, or any 3D training supervision. Experiments demonstrate that MetricHMR achieves state-of-the-art in both local motion and global trajectory estimation.

**Limitations.** In the inference process, for images with known intrinsics, we rely on the performance of UniDepth and thus are unable to handle the failure cases of UniDepth.

## References

- [1] Shariq Farooq Bhat, Reiner Birkel, Diana Wofk, Peter Wonka, and Matthias Müller. Zoedepth: Zero-shot transfer by combining relative and metric depth. *arXiv preprint arXiv:2302.12288*, 2023. **3**
- [2] Federica Bogo, Angjoo Kanazawa, Christoph Lassner, Peter Gehler, Javier Romero, and Michael J. Black. Keep it smpl: Automatic estimation of 3d human pose and shape from a single image. In *Proceedings of the European Conference on Computer Vision*, pages 561—578, 2016. **1, 2**
- [3] Zhongang Cai, Wanqi Yin, Ailing Zeng, Chen Wei, Qingping Sun, Wang Yanjun, Hui En Pang, Haiyi Mei, Mingyuan Zhang, Lei Zhang, et al. Smpler-x: Scaling up expressive human pose and shape estimation. *Conference on Neural Information Processing Systems*, 36, 2024. **1, 2**
- [4] Sai Kumar Dwivedi, Yu Sun, Priyanka Patel, Yao Feng, and Michael J Black. Tokenhmr: Advancing human mesh recovery with a tokenized pose representation. In *Proceedings of the IEEE conference on computer vision and pattern recognition*, pages 1323–1333, 2024.
- [5] Shubham Goel, Georgios Pavlakos, Jathushan Rajasegaran, Angjoo Kanazawa, and Jitendra Malik. Humans in 4d: Reconstructing and tracking humans with transformers. In *Proceedings of the IEEE international conference on computer vision*, pages 14783–14794, 2023. **1, 2, 3**
- [6] Riza Alp Guler and Iasonas Kokkinos. Holopose: Holistic 3d human reconstruction in-the-wild. In *Proceedings of the IEEE/CVF Conference on Computer Vision and Pattern Recognition*, pages 10876–10886, 2019. **2**
- [7] Catalin Ionescu, Dragos Papava, Vlad Olaru, and Cristian Sminchisescu. Human3.6m: Large scale datasets and predictive methods for 3d human sensing in natural environments. *IEEE transactions on pattern analysis and machine intelligence*, 36(7):1325–1339, 2013. **6**

- [8] Angjoo Kanazawa, Michael J Black, David W Jacobs, and Jitendra Malik. End-to-end recovery of human shape and pose. In *Proceedings of the IEEE conference on computer vision and pattern recognition*, pages 7122–7131, 2018. [1](#), [2](#), [3](#), [6](#)
- [9] Manuel Kaufmann, Jie Song, Chen Guo, Kaiyue Shen, Tianjian Jiang, Chengcheng Tang, Juan José Zárate, and Otmar Hilliges. Emdb: The electromagnetic database of global 3d human pose and shape in the wild. In *Proceedings of the IEEE/CVF International Conference on Computer Vision*, pages 14632–14643, 2023. [7](#)
- [10] Muhammed Kocabas, Nikos Athanasiou, and Michael J. Black. Vibe: Video inference for human body pose and shape estimation. In *Proceedings of the IEEE conference on computer vision and pattern recognition*, pages 5252–5262, 2020. [1](#), [2](#)
- [11] Muhammed Kocabas, Chun-Hao P Huang, Joachim Tesch, Lea Müller, Otmar Hilliges, and Michael J Black. Spec: Seeing people in the wild with an estimated camera. In *Proceedings of the IEEE/CVF International Conference on Computer Vision*, pages 11035–11045, 2021. [3](#)
- [12] Muhammed Kocabas, Ye Yuan, Pavlo Molchanov, Yunrong Guo, Michael J Black, Otmar Hilliges, Jan Kautz, and Umar Iqbal. Pace: Human and camera motion estimation from in-the-wild videos. In *2024 International Conference on 3D Vision (3DV)*, pages 397–408. IEEE, 2024. [6](#)
- [13] Nikos Kolotouros, Georgios Pavlakos, Michael J Black, and Kostas Daniilidis. Learning to reconstruct 3d human pose and shape via model-fitting in the loop. In *Proceedings of the IEEE international conference on computer vision*, pages 2252–2261, 2019. [1](#), [2](#), [3](#)
- [14] Zhihao Li, Jianzhuang Liu, Zhensong Zhang, Songcen Xu, and Youliang Yan. Cliff: Carrying location information in full frames into human pose and shape estimation. In *Proceedings of the European Conference on Computer Vision*, pages 590–606, 2022. [1](#), [2](#), [3](#), [4](#), [5](#), [6](#)
- [15] Tsung-Yi Lin, Michael Maire, Serge Belongie, James Hays, Pietro Perona, Deva Ramanan, Piotr Dollár, and C Lawrence Zitnick. Microsoft coco: Common objects in context. In *Proceedings of the European Conference on Computer Vision*, pages 740–755. Springer, 2014. [7](#)
- [16] Matthew Loper, Naureen Mahmood, Javier Romero, Gerard Pons-Moll, and Michael J Black. Smpl: A skinned multi-person linear model. *ACM Trans. Gr.*, 34(6):1–16, 2015. [5](#)
- [17] Dushyant Mehta, Helge Rhodin, Dan Casas, Pascal Fua, Oleksandr Sotnychenko, Weipeng Xu, and Christian Theobalt. Monocular 3d human pose estimation in the wild using improved cnn supervision. In *2017 international conference on 3D vision (3DV)*, pages 506–516. IEEE, 2017. [6](#)
- [18] Lea Müller, Ahmed A. A. Osman, Siyu Tang, Chun-Hao P. Huang, and Michael J. Black. On self-contact and human pose. In *Proceedings of the IEEE/CVF Conference on Computer Vision and Pattern Recognition*, pages 9990–9999, 2021. [4](#)
- [19] Georgios Pavlakos, Vasileios Choutas, Nima Ghorbani, Timo Bolkart, Ahmed AA Osman, Dimitrios Tzionas, and Michael J Black. Expressive body capture: 3d hands, face, and body from a single image. In *Proceedings of the IEEE conference on computer vision and pattern recognition*, pages 10975–10985, 2019. [2](#)
- [20] Duc-Hai Pham, Tung Do, Phong Nguyen, Binh-Son Hua, Khoi Nguyen, and Rang Nguyen. Sharpdepth: Sharpening metric depth predictions using diffusion distillation. *arXiv preprint arXiv:2411.18229*, 2024. [2](#), [3](#)
- [21] Luigi Piccinelli, Yung-Hsu Yang, Christos Sakaridis, Mattia Segu, Siyuan Li, Luc Van Gool, and Fisher Yu. Unidepth: Universal monocular metric depth estimation. In *Proceedings of the IEEE conference on computer vision and pattern recognition*, pages 10106–10116, 2024. [2](#), [3](#), [4](#), [5](#), [7](#)
- [22] István Sáráncsi and Gerard Pons-Moll. Neural localizer fields for continuous 3d human pose and shape estimation. *Conference on Neural Information Processing Systems*, 37:140032–140065, 2025. [1](#)
- [23] Zehong Shen, Huaijin Pi, Yan Xia, Zhi Cen, Sida Peng, Zechen Hu, Hujun Bao, Ruizhen Hu, and Xiaowei Zhou. World-grounded human motion recovery via gravity-view coordinates. In *SIGGRAPH Asia 2024 Conference Papers*, pages 1–11, 2024. [1](#), [3](#), [6](#)
- [24] Soyong Shin, Juyong Kim, Eni Halilaj, and Michael J Black. Wham: Reconstructing world-grounded humans with accurate 3d motion. In *Proceedings of the IEEE conference on computer vision and pattern recognition*, pages 2070–2080, 2024. [1](#), [3](#), [6](#)
- [25] Yu Sun, Wu Liu, Qian Bao, Yili Fu, Tao Mei, and Michael J Black. Putting people in their place: Monocular regression of 3d people in depth. In *Proceedings of the IEEE conference on computer vision and pattern recognition*, pages 13243–13252, 2022. [3](#)
- [26] Yu Sun, Qian Bao, Wu Liu, Tao Mei, and Michael J Black. Trace: 5d temporal regression of avatars with dynamic cameras in 3d environments. In *Proceedings of the IEEE conference on computer vision and pattern recognition*, pages 8856–8866, 2023. [1](#), [3](#), [6](#), [7](#)
- [27] Zachary Teed and Jia Deng. Droid-slam: Deep visual slam for monocular, stereo, and rgb-d cameras. *Advances in neural information processing systems*, 34:16558–16569, 2021. [3](#), [7](#)
- [28] Zachary Teed, Lahav Lipson, and Jia Deng. Deep patch visual odometry. *Advances in Neural Information Processing Systems*, 36:39033–39051, 2023. [7](#)
- [29] Timo Von Marcard, Roberto Henschel, Michael J Black, Bodo Rosenhahn, and Gerard Pons-Moll. Recovering accurate 3d human pose in the wild using imus and a moving camera, 2018. [6](#), [7](#)
- [30] Shengze Wang, Jiefeng Li, Tianye Li, Ye Yuan, Henry Fuchs, Koki Nagano, Shalini De Mello, and Michael Stengel. Blade: Single-view body mesh learning through accurate depth estimation. *arXiv preprint arXiv:2412.08640*, 2024. [3](#), [6](#)
- [31] Wenjia Wang, Yongtao Ge, Haiyi Mei, Zhongang Cai, Qingping Sun, Yanjun Wang, Chunhua Shen, Lei Yang, and Taku Komura. Zolly: Zoom focal length correctly for perspective-distorted human mesh reconstruction. In *Proceedings of the IEEE international conference on computer vision*, pages 3925–3935, 2023. [3](#)

- [32] Yufu Wang, Ziyun Wang, Lingjie Liu, and Kostas Daniilidis. Tram: Global trajectory and motion of 3d humans from in-the-wild videos. In *Proceedings of the European Conference on Computer Vision*, pages 467–487. Springer, 2024. 3, 6
- [33] Donglai Xiang, Hanbyul Joo, and Yaser Sheikh. Monocular total capture: Posing face, body, and hands in the wild. In *Proceedings of the IEEE/CVF Conference on Computer Vision and Pattern Recognition*, pages 10957–10966, 2019. 2
- [34] Lihe Yang, Bingyi Kang, Zilong Huang, Zhen Zhao, Xiaogang Xu, Jiashi Feng, and Hengshuang Zhao. Depth anything v2. *Advances in Neural Information Processing Systems*, 37:21875–21911, 2024. 2, 3, 4
- [35] Vickie Ye, Georgios Pavlakos, Jitendra Malik, and Angjoo Kanazawa. Decoupling human and camera motion from videos in the wild. In *Proceedings of the IEEE/CVF conference on computer vision and pattern recognition*, pages 21222–21232, 2023. 3, 6
- [36] Wei Yin, Chi Zhang, Hao Chen, Zhipeng Cai, Gang Yu, Kaixuan Wang, Xiaozhi Chen, and Chunhua Shen. Metric3d: Towards zero-shot metric 3d prediction from a single image. In *Proceedings of the IEEE international conference on computer vision*, pages 9043–9053, 2023. 2, 3, 4
- [37] Hongwen Zhang, Yating Tian, Xinchu Zhou, Wanli Ouyang, Yebin Liu, Limin Wang, and Zhenan Sun. Pymaf: 3d human pose and shape regression with pyramidal mesh alignment feedback loop. In *Proceedings of the IEEE international conference on computer vision*, pages 11446–11456, 2021. 1, 2, 3
- [38] Hongwen Zhang, Yating Tian, Yuxiang Zhang, Mengcheng Li, Liang An, Zhenan Sun, and Yebin Liu. Pymaf-x: Towards well-aligned full-body model regression from monocular images. *IEEE Transactions on Pattern Analysis and Machine Intelligence*, 45(10):12287–12303, 2023. 1, 2
- [39] Yizhou Zhao, Hengwei Bian, Kaihua Chen, Pengliang Ji, Liao Qu, Shao-yu Lin, Weichen Yu, Haoran Li, Hao Chen, Jun Shen, et al. Metric from human: Zero-shot monocular metric depth estimation via test-time adaptation. In *The Thirty-eighth Annual Conference on Neural Information Processing Systems*, 2024. 3